

## ASEISMIC EFFECT OF GEOTECHNICAL IMPROVEMENT FOR TYPICAL QUAY WALLS

T HYODO<sup>1</sup>, T AKIYOSHI<sup>2</sup>, H MATSUMOTO<sup>3</sup> And K FUCHIDA<sup>4</sup>

### SUMMARY

Shaking table tests and effective stress analyses were carried out to analyze the failure modes of typical quaywalls and investigate the aseismic effect of geotechnical improvement for prevention of the permanent displacement. As a result, before the improvement by compaction method, displacement of gravity-caisson-type quaywall is most dependent on the backfill earth pressure. After the improvement, the earth pressure and pore water pressure don't increase in spite of the high initial earth pressure. The improvement at the backfill of sheet pile quaywall by gravel-drained method depresses the excess pore water pressure and the displacement as well. It is concluded that the displacement of these types of quaywall are the most dependent on liquefaction at the backfill, and therefore these geotechnical improvements are quite effective to prevent liquefaction.

### INTRODUCTION

There have been various developments of countermeasures for liquefaction of the sand deposits so far, which would be advantageous in soft grounds such as artificial islands or reclaimed grounds. Although liquefaction occurred widely around port and harbor facilities during the 1995 Hyogoken-Nambu earthquake, there were little damages at the sites where improved by compaction methods or drain methods[Yasuda, Ishihara, Harada and Shinkawa, 1996]. As this the field data have proved that geotechnical improvements would effectively reduce the liquefaction-induced damages. The mechanism of prevention effects on quaywalls by these countermeasures, however, has been hardly revealed so far.

In structural aspects, gravity-caisson-type and sheet-pile-type, which are the most typical types of quaywall in Japan, have been utilized widely in waterfront projects because of its simplified composition, reliability and reasonable cost. In static principle, gravity-caisson-type quaywalls support the backfill pressure by the frictional force at the bottom surface, and sheet-pile-type quaywalls generally bear the backfill pressure by the bending moment reaction of piles installed into rigid base layer. These types of quaywall are currently designed by using pseudo static methods with seismic coefficients. However, actual seismic response of structures is very complex due to the dynamic soil-structure interaction and gradual changes of characteristics of soil around the structures.

<sup>1</sup> Tech Research Inst, Civil Engineering Division, Wakachiku Construction Co. Ltd., Japan Email: hyodo@wakachiku.co.jp

<sup>2</sup> Department of Civil Engineering and Architecture, Kumamoto University, Japan Email: akiyoshi@gpo.kumamoto-u.ac.jp

<sup>3</sup> Department of Civil Engineering and Architecture, Kumamoto University, Japan Email: akiyoshi@gpo.kumamoto-u.ac.jp

<sup>4</sup> Dept of Civil and Architectural Eng, Yatsushiro College of Technology, Japan Email: fuchida@as.yatsushiro-uct.ac.jp

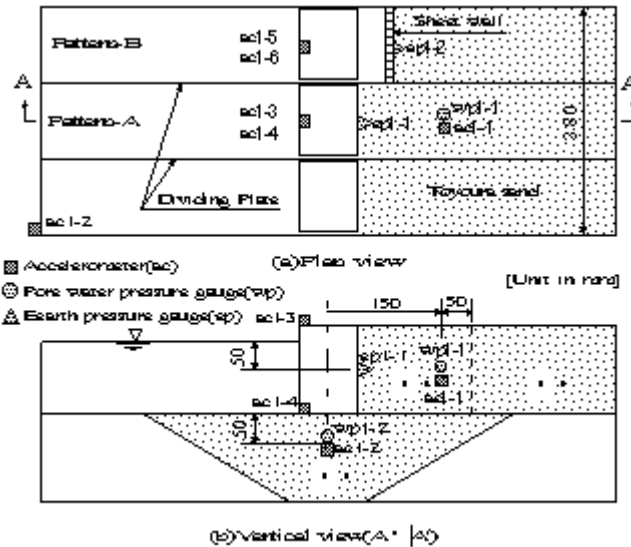


Figure 1 : The plan and vertical view of gravity-caisson type quaywall model

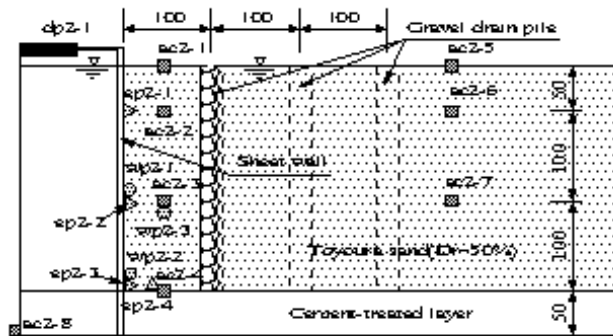


Figure 2 : The cross section of sheet-pile-type quaywall model

Thus, this study aims to analyze the failure modes of typical quaywalls experimentally and theoretically due to strong ground shaking, and to show the seismic effect of geotechnical improvements on the prevention of the permanent displacement.

### SHAKING TABLE TESTS

A series of shaking table tests were performed in gravitational field to investigate the mechanism of movement of quaywall and to obtain the optimum improvement area for minimizing liquefaction-induced damages. The similitude rule in gravitational field for soil-structure-fluid [Iai, 1989] was adopted for the series of model tests which were scaled to 1/100 geometrically for real structures, and the scaling factors are listed in **Table 1**. In order to match the permeability between model and prototype soil, the methyl-cellulose solution was used as the pore fluid and adjusted viscosity.

**Figure 1** shows a typical plan and vertical view of the gravity-caisson-type model, and **Figure 2** the cross section of the sheet-pile-type model. Both figures also include the locations of sensors used for the measurement of acceleration, pore water pressure and earth pressure during dynamic shaking. The sand box was set up on the shaking table. The sand box for the gravity-caisson-type model was divided into 3 blocks by vertical plates. For Pattern-A, the caisson and the saturated soil were placed at the middle block and touches each other, which is the most popular cases as shown in **Figure 1**. For Pattern-B, the caisson was placed at the side block and separated by the sheet wall to measure the backfill pressure directly, where the gap between the caisson and sheet wall was 40mm. A dummy caisson was placed at the rest block for the counter weight. A caisson model was the cement mortar block of 100mm long, 120mm wide and 150mm in height. In the sheet-pile-type model tests, the sheet pile made of acrylic was fixed into the cement-mixed rigid base layer.

The Toyoura sand was used as the sand deposits in both types of model tests. In the series of gravity-caisson-type tests, the loose sand deposit of the relative density  $D_r$  of 50% was produced by the water deposition method and the dense ground as a unliquefiable layer was made by tamping to the relative density  $D_r$  of 80%. In the series of sheet-pile-type tests, the loose backfill ground was also set with relative density  $D_r$  of 50%, in which the 7th-gravel in the grain size standard was used as the drain material. The diameter of gravel-pile was 30mm and the pile-spacing was 100mm in width as shown in **Figure 2**. Initially, some noodles were set up vertically on the side glass wall of the sand box in order to observe the lateral displacement of backfill soil after shaking. In order to facilitate the comparison with the analytical results, the test results are presented in prototype scale. Sinusoidal waves were input at the bottom of sand box in the normal direction of the quaywall face line, in which the peak accelerations were  $1.50\text{m/s}^2$  in the series of gravity-caisson-type tests, and  $1.30\text{m/s}^2$  in the series of sheet-pile-type tests. A total of ten model tests were carried out under various conditions as listed in **Table 2**.

### EFFECTIVE STRESS ANALYSIS

The 2D FE program for effective stress analysis "FLIP"[Iai, Matsunaga and Kameoka, 1992], which is based on the two phase mixture theory and the multiple shear mechanism was defined in the plane strain conditions, was used for the simulation of the model tests in order to investigate the details of the mechanism of lateral

**Table 1 : Test cases**  
(a)Gravity-caisson-type      (b)Sheet-pile-type

| Items               | Scaling factors in general (prototype/model) | Scaling factors for model tests |
|---------------------|--|---------------------------------|
| length              | $f \tilde{E}$                                | 100                             |
| density             | 1  | 1                               |
| time                | $f \tilde{E}^{0.75}$                         | 31.6                            |
| stress              | $f \tilde{E}$                                | 100                             |
| pore water pressure | $f \tilde{E}$                                | 100                             |
| permeability        | $f \tilde{E}^{0.75}$                         | 31.6                            |
| displacement        | $f \tilde{E}^{0.50}$                         | 1000                            |
| velocity            | $f \tilde{E}^{0.75}$                         | 31.6                            |
| acceleration        | 1  | 1                               |

**Table 2 : Model parameters for FLIP analysis**

|         | Compacted area |         | Total number of gravel drain pile lines | Distance from sheet wall(mm) |
|---------|----------------|---------|---|------------------------------|
| Case1-1 | unimproved     | Case2-1 | unimproved                              |                              |
| Case1-2 | a              | Case2-2 | 1                                       | 100                          |
| Case1-3 | a,b            | Case2-3 | 1                                       | 300                          |
| Case1-4 | c              | Case2-4 | 2                                       | 100,200                      |
|         |                | Case2-5 | 2                                       | 200,300                      |
|         |                | Case2-6 | 2                                       | 100,300                      |

Locations of a,b,c are referred in Figure 1

**Table 3 : Model parameters for FLIP analysis**

| Parameters        |   | Unimproved (Dr=50%) | Compacted (Dr=80%) | Gravel-Drained |
|-------------------|---|---------------------|--------------------|----------------|
| $K_{ma}$          | Rebound modulus                                     | 210,600 kPa         | 388,500 kPa        | 256,000kPa     |
| $G_{ma}$          | Shear modulus                                       | 80,700 kPa          | 149,000 kPa        | 96,200kPa      |
| $f \tilde{\phi}'$ | Shear resistance angle                              | 37.0                | 43.0               | 39.6           |
| $h_{max}$         | Hysteric damping factor at large shear strain level | 0.24                | 0.24               | 0.24           |
| $p_1$             | Initial phase of dilatancy                          | 0.50                | 0.50               |                |
| $p_2$             | Final phase of dilatancy                            | 1.35                | 0.70               |                |
| $w_1$             | Overall dilatancy                                   | 10.0                | 22.5               |                |
| $S_1$             | Ultimate limit of dilatancy                         | 0.005               | 0.005              |                |
| $c_1$             | Threshold limit                                     | 1.00                | 1.00               |                |
| $f \tilde{\phi}'$ | Phase transformation angle                          | 28.0                | 28.0               |                |

deformation of soil and the effect of geotechnical improvement for backfills. FLIP has been often used in the seismic problems and succeeded to deal well with soil-structure interaction especially including liquefaction effects, and shown the efficiency in recent several field studies [Tai, Ichii, Liu and Morita, 1998], [Yuasa, Yasunaka and Adachi, 1998].

**Table 3** lists the specific values of parameters used for FLIP analyses, where the dynamical soil parameters were calculated with a simplified method proposed by Morita *et al.* [Morita, Iai, Liu, Ichii and Sato, 1997], and the numerical simulation by using cyclic tri-axial test results determined the dilatancy parameters of sand deposit.

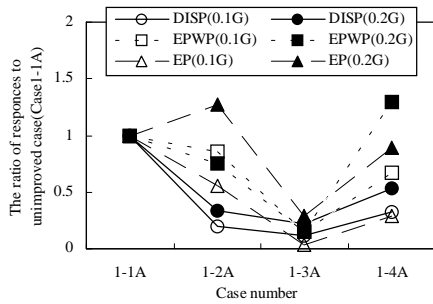


**Figure 4 : Residual movement of caisson in Pattern-A (Analyses, Acc.max= 0.2G)**

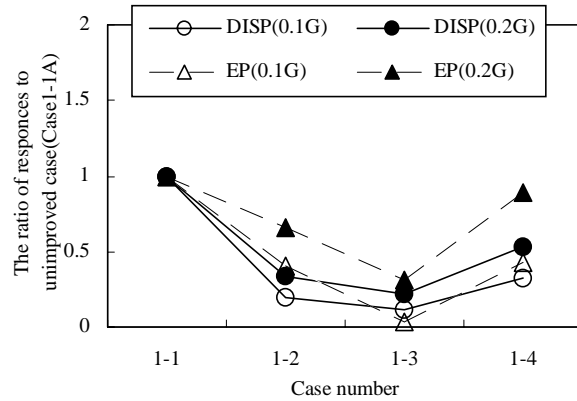


**Figure 3 : The ratio of peak response to unimproved case (Model tests)**

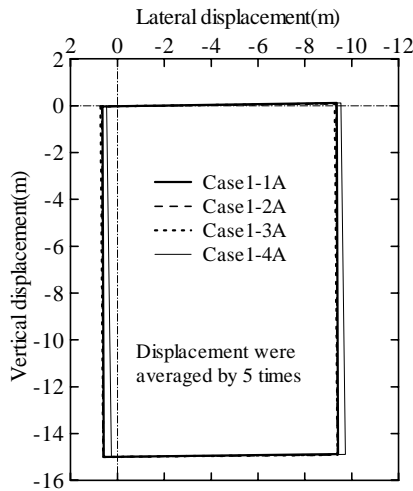


**Figure 5 : Distribution of excess pore water pressure ratio (Analyses, Acc.max=0.1G)**

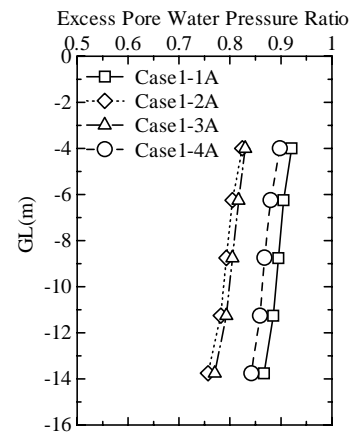


**Figure 6 : Relationship between earth pressure and lateral displacement of caisson (Model tests)**

The area improved by gravel-drained method was assumed to be of unliquefiable material, and initial shear modulus of gravel-drained area  $G_0$  was defined by following formula :

$$G_0 = A_s \cdot G_{0g} + (1 - A_s) G_{0s} \quad (1)$$

where  $A_s$  is the ratio of pile diameter to pile spacing, and  $G_{0g}, G_{0s}$  are initial shear modulus of gravel pile and sand deposit, respectively. First, a static analyses were performed under drained conditions in order to simulate the stress conditions before strong shaking, and then the results were used for the initial condition of dynamic analysis. The dynamic analyses were performed under undrained conditions to approximate the saturated soil behavior in field. The equivalent viscous dampers were set at both lateral boundaries and at the bottom boundary during shaking.

## RESULTS OF MODEL TESTS AND ANALYSES

### Gravity-caisson-type quaywall

Since the results of model tests for gravity-caisson-type have been mostly concluded in previous study [Hyodo, Akiyoshi, Fuchida and Imanaka, 1998], this section shows the outline of the test results. In order to show the effect of the compaction method, the ratio of caisson's peak responses to are plotted in **Figure 3**, where the peak responses were measured lateral displacement at the top of the caisson or excess pore water pressure ratio. The lateral displacement (DISP in the diagram) of caisson after shaking was small especially for the case of Case1-3A, in which the subscript A means the series of the Pattern-A, and B the Pattern-B. These results illustrate that there exists an optimal place for the construction of the compaction piles for minimizing the caisson displacement. The excess pore water pressure (EPWP in the diagram) just behind the caisson wall in Case1-4A of the case of the improved foundation underneath the caisson was higher than unimproved case (Case1-1A) despite of the similar tendency to the lateral displacement of caisson. Earth pressure (EP in the diagram) also shows the minimum response for the Case1-3A.

**Figure 4** shows the good agreement between the earth pressure at the top of the sheet pile in the Pattern-B and the lateral displacement of the caisson in Pattern-A. Since the lateral deformation of the backfill was not allowed at all in Pattern-B due to fixed sheet wall, earth pressure increment induced by the backfill liquefaction mainly leads to increment of the movement of caisson.

**Figure 5** shows the residual movement of caisson in Pattern-A. Clear tendency due to the experimental Patterns can not be seen.

**Figure 6** shows that the excess pore water pressure ratio in the backfill ranges from 0.75 to 0.95, which means 4 cases almost liquefied. For this simple uniform soil profile of the backfill, the compaction pile method cannot prevent liquefaction.

### Sheet-pile-type quaywall

In the seismic behavior of sheet-pile-type quaywall, the effect of its inertia force is much smaller than gravity-caisson-type quaywall. Hence, it was quite important to analyze the effects of the generation of the excess pore water pressure on the total earth pressure increment in the backfill during strong shaking. If the backfill liquefied completely, the increase of total earth pressure  $\Delta p$  is given by following formula :

$$\Delta p = (1 - K) \gamma' z \quad (2)$$
 where  $K$  is the coefficient of earth pressure,  $\gamma'$  the sub-merged density and  $z$  the depth. According to the test results of measurement, the coefficient of earth pressure  $K$  in model tests ranged from 0.3 to 0.5.

**Figure 7** shows the time histories of total earth pressure, excess pore water pressure ratio (EPWP) and lateral displacement at the top of sheet pile. Earth pressure in this figure denotes the increment of total stress including water pressure. According to the comparison of each responses, the difference of earth pressure increment at the upper layer (ep2-1 and ep2-2) between Case2-1 and Case2-2 is hardly clarified. There is, however, a tendency of gradual increment of earth pressure after 100 seconds past in Case2-1. On the other hand, earth pressure behaves almost level after 100 seconds past in Case2-2. In both cases, the excess pore water pressure at the upper layer of the backfill (wp2-1 and wp2-3) recovers quickly and drastically to the level of initial effective overburden pressure after 60 seconds past. On the other hand, the excess pore water pressure at the bottom layer of the backfill (wp2-2) did not reach the level of the initial effective overburden pressure in spite of long time shaking.

**Figure 8** illustrates the comparison of residual lateral displacement of backfill ground between unimproved Case2-1 and gravel-drained Case2-2 by the observation of the noodles, and shows that the backfill ground of the unimproved Case2-1 deformed larger than the gravel-drained Case2-2. Although this result demonstrates that the gravel-drained method applied in the backfill is useful for reducing the liquefaction-induced lateral displacement, the dissipation effect of gravel drain pile appears after a few seconds in these model conditions.

**Figure 9** illustrates the residual deformation of the backfill ground measured with the movement of noodles,

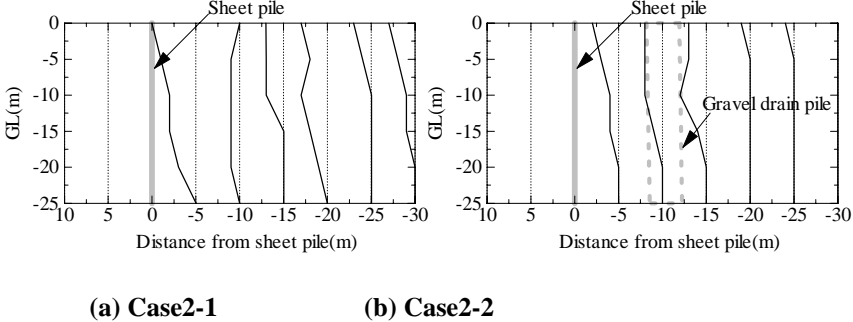


**Figure 8 : Comparison of lateral displacement after shaking (Model tests)**

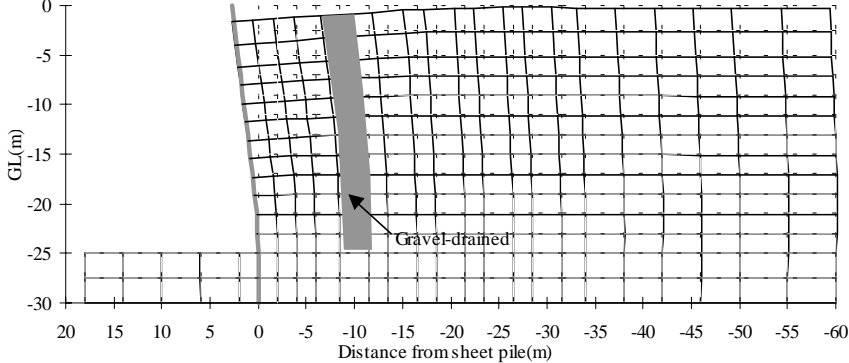


**Figure 9 : Deformation of sheet-pile-type quaywall after shaking (Analysis, Case2-2)**

where dot lines and solid lines indicate before and after shaking, respectively. It shows that the surface layer of the backfill deformed larger than bottom layer and that the noodles moved toward the nearest drainage pile due to seepage flow. The results reveals that drainage piles gradually dissipate excess pore water pressure and to restraint backfill deformation due to lateral permanent spreading of soil.

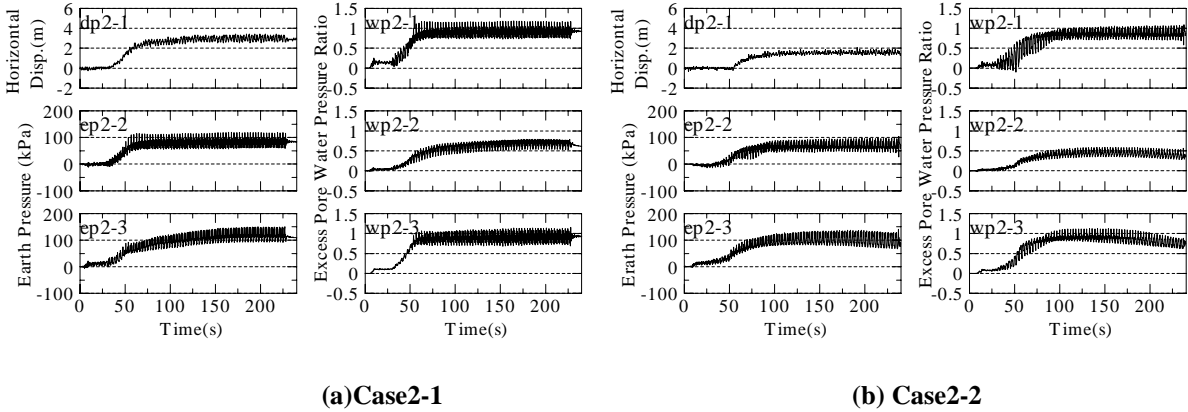


**Figure 7 : Time histories (Earth pressure, Excess pore water pressure ratio and Lateral displacement at the top of sheet pile)**

The peak lateral displacement at the top of sheet pile were plotted in **Figure 10**. The results of analyses are approximately 20% smaller compared to the model test results.

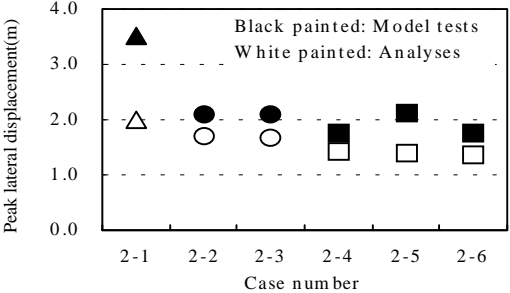
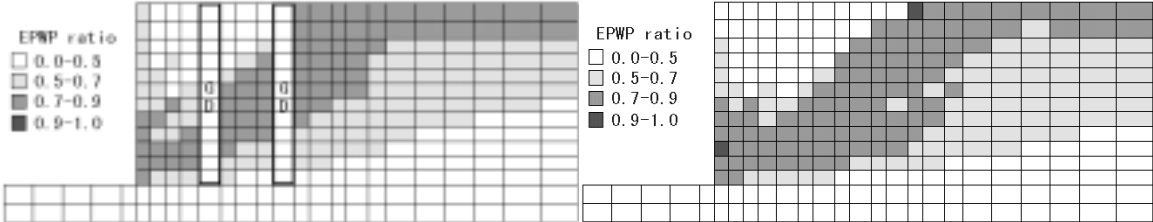
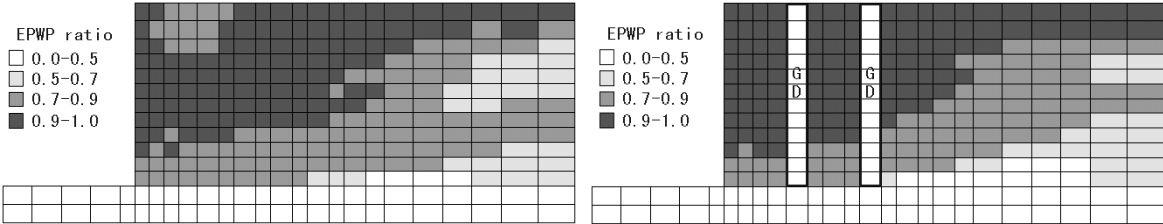


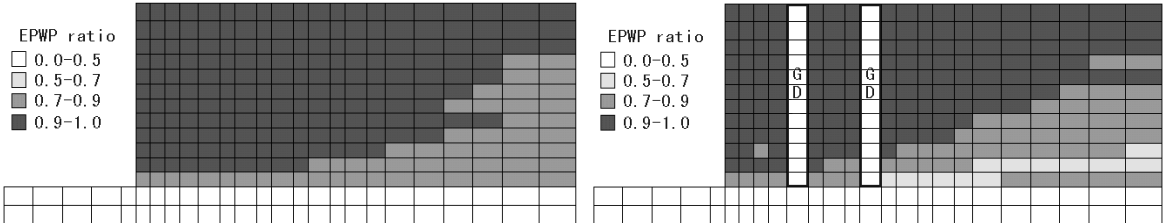
**Figure 11 : Peak lateral displacement (Model tests and Analyses)**



**At time of 1 second after excitation**



**At time of 2 seconds after excitation**



**At time of 5 seconds after excitation**

**(a)Case2-1(Unimproved)**

**(b)Case2-4(Gravel-drained)**

**Figure 10 : Distribution of excess pore water pressure ratio  $(1 - \sigma'_m / \sigma'_{m0})$**

In order to discuss the details on the mechanism of the sheet pile movement, the distributions of the excess pore water pressure ratio  $(1 - \sigma'_m / \sigma'_{m0})$  at the time step in the case of Case2-1 and Case2-4 are shown in **Figure 11**,

in which  $\sigma'_m, \sigma'_{m0}$  are the current mean effective stress and the initial mean effective stress, respectively. As mentioned earlier, since all analyses were performed under undrained conditions, the effect of drainage of gravel drain piles during shaking were not considered in this procedure. Besides, since the shear modulus of gravel-drained area were assumed to be adjusted defined by **Equation 1**, numerical results of gravel-drained cases seem to be the same distribution of pore water pressure as the unimproved case. However, higher excess pore water pressure distributes at the deep area of the backfill in the unimproved cases. The bending moment distribution of sheet pile, shown in **Figure 12**, reveals the main cause of caisson's displacement due to the earth pressure increment induced by liquefaction. It is noted that the values of bending moment would not be computed correctly because the sheet pile is assumed to be elastic beam elements in this analyses.

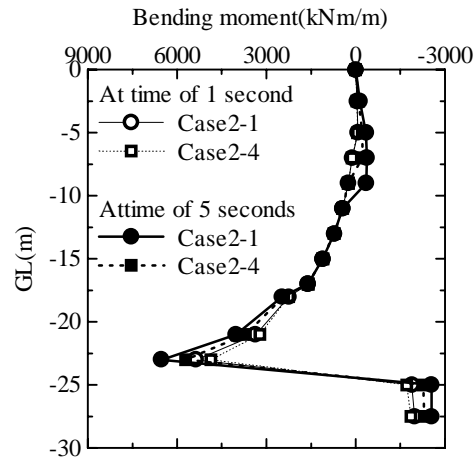


**Figure 12 : Distribution of bending moment acting on sheet pile (Analyses)**

## CONCLUSIONS

The results of this study are concluded as follows.

1. The lateral displacement of quaywalls was mainly induced by earth pressure increment due to the quick generation of excess pore water pressure.
2. It was clarified experimentally that the compaction method adopted in the backfill is more effective for preventing the lateral movement of gravity-caisson-type quaywall because of the improvement of soil stiffness and the prevention of generation of excess pore water pressure, and that the gravel-drained method used for the backfill improvement is also effective due to the well drainage of excess pore water pressure during strong shaking.
3. Some numerical case studies by effective stress analysis demonstrated that compaction method used in the backfill is the same tendency of effects to depress the excess pore water pressure as the test results, and that gravel-drained method is more effective to reduce the excess pore water pressure at the deep area in backfill than unimproved case.

## REFERENCES

1. Yasuda, S., Ishihara, K., Harada, K. and Shinkawa, N. (1996), "Effect of Soil Improvement on Ground Subsidence due to Liquefaction," *Soils and Foundations*, Special Issue on Geotechnical Aspects of the January 17 1995 Hyogoken-Nambu Earthquake, pp99-108 (in Japanese).
2. Iai, S. (1989), "Similitude for shaking table tests on soil-structure-fluid model in 1 g gravitational field," *Soils and Foundations*, 29, 1, pp105-118 (in Japanese).
3. Iai, S., Matsunaga, Y. and Kameoka, T. (1992), "Strain space plasticity model for cyclic mobility," *Soils and Foundations*, 32, 2, pp.1-15 (in Japanese).
4. Iai, S., Ichii, K., Liu, H. and Morita, T. (1998), "Effective stress analysis of port structures," *Soils and Foundations*, Special Issue on Geotechnical Aspects of the January 17 1995 Hyogoken-Nambu Earthquake, 2, pp97-114 (in Japanese).
5. Yuasa, A., Yasunaka, M. and Adachi, M.(1998), "Effective Stress Analysis on an Embankment Dam Damaged by Liquefaction," *Proc. The 10th Japan Earthquake Engineering Symposium*, pp1349-1354.
6. Morita, T., Iai, S., Liu, H., Ichii, K. and Sato, Y.(1997), "Simplified Method to Determine Parameter of FLIP," *Report of the port and harbour research institute*, 869 (in Japanese).
7. Hyodo, T., Akiyoshi, T., Fuchida, K. and Imanaka, Y.(1998), "Effects of Soil Improvement on Seismic Earth Pressure Acting on Gravity-type Quay Walls," *Proc. The 10th Japan Earthquake Engineering Symposium*, pp1781-1784.